A study of Fermi hole and partial Fermi hole for Li- and C-Atoms in different states *1s 2p, 1s 3p, 1s 3d* and *2s 2p*

Ali. A. Alzubadi[1], Khalil H. AL-Bayati[2], Naeemah Ch. M.[2]

[1]Physics Department, College of Science, University of Baghdad.

[2]Physics Department, College of Science for Women, University of Baghdad.

E-mail: na_ch_ma@yahoo.com

Abstract

The electron correlation effect for inter-shell have been analysed in terms of Fermi hole and partial Fermi hole for Li-atom in the excited states $(1s^2\ 3p)$ and $(1s^2\ 3d)$ using Hartree-Fock approximation (HF). Fermi hole $\Delta f(r_{12})$ and partial Fermi hole $\Delta g(r_{12}, r_1)$ were determined in position space. Each plot of the physical properties in this work is normalized to unity. The calculation was performed using Mathcad 14 program.

Key words

Fermi hole, Partial Fermi hole, electron correlation.

Article info.

Received: Oct. 2014
Accepted: Dec. 2014
Published: Sep. 2015

دراسة فجوة فيرمي وفجوة فيرمي الجزئية لذرتي الليثيوم والكاربون في حالات مختلفة *1s 3d، 1s 3p ، 1s 2p و 2s 2p*

علي عبد اللطيف كريم الزبيدي[1]، خليل هادي أحمد البياتي[2]، نعيمة جيجان مذكور[2]

[1]قسم الفيزياء، كلية العلوم، جامعة بغداد

[2]قسم الفيزياء، كلية العلوم للبنات، جامعة بغداد

الخلاصـــة

تم تحليل الترابط الألكتروني للاغلفة البينية من خلال فجوة فيرمي وفجوة فيرمي الجزئية لذرة الليثيوم في الحالات المتهيجة $(1s^2\ 3p)$ و $(1s^2\ 3d)$ بأستخدام الدالة التقريبية لهارتي-فوك (HF). تم تحديد فجوة فيرمي $\Delta f(r_{12})$ وفجوة فيرمي الجزئية $\Delta g(r_{12}, r_1)$ في الفضاء المكاني. كل رسم للخصائص الفيزيائية في هذا البحث يحقق شرط العيارية للواحد. الحسابات تم تنفيذها باستخدام برنامج Mathcad 14.

Introduction

The electron correlation in an atom or molecule is of two kinds, due to Coulomb and exchange interaction. In the first of these, the classical Coulomb repulsion between each pair of electrons which have different spins, leads to the formation of a hole in the atomic or molecular charge cloud around each chosen electron which is called a Coulomb hole [1]. The second kind, the interaction of electrons with parallel spins which keeps the electrons apart and lead to the Fermi hole (it is also known as the exchange hole) which arises from the nature of fermions The first numerical calculations for the

Fermi hole in atoms were reported by Maslen (1956) [2] and Sperber (1971)[3]. The Fermi hole was defined quantitatively in terms of pair distribution functions by Boyd and Coulson 1974 [4]. Explict calculations of Boyd and Coulson 1974, Moiseyev et al. 1975 [5] for the 2^3s state of the helium isoelectronic sequence and the ground state of beryllium have provided a simple physical picture of the average Fermi hole in the charge cloud around any chosen electron in simple atomic systems. The electron correlation has been examined within inter-shell for a series of Li-like ions in their excited state *(1s^2 3s)* comparing with *(1s^2 2p)* by AL-Bayati (1985) [6]. Inter-shell descriptions were obtained at a Hartree-Fock (HF) level from Weiss 1963 [7]. The Fermi and Coulomb holes that can be used to describe the physics of electron correlation are calculated and analysed for a number of typical cases, ranging from prototype dynamical correlation to purely nondynamical correlation by Buijse & Baerends (2002) [8], and Fermi hole has studied for the configurations 1s 2p and $2p^2$ for He atom where the Pauli principle was satisfied by Dan Dill (2003) [9]. Partitioning the second-order density into its pairwise components, correlation effects were then analyzed in terms of Fermi hole $\Delta f(r_{12})$ and partial Fermi hole $g(r_{12}, r_1)$ in *(1s^2 3s)* and *(1s^2 3p)* states by Ali A. Alzubadi 2005 [10]. In the present reseearch, the analysis is extended here to the third and fourth excited states of the Li-atom *(1s^2 3p)* and *(1s^2 3d)*. Moreover, since the third and fourth excited states have a none-zero total angular momentum, a comparison of its correlation properties with those for the ground state of *S* symmetry, will be of special interest.

Theory and methodology

HF wave function is appropriate for many different applications in electron structure theory. It describe the internal dynamics of an N-electron atom in the internal spatial coordinates and the spin coordinates and given by

$$\Psi(\vec{r}_1,\vec{r}_2,...,\vec{r}_A)=\frac{1}{\sqrt{A!}}\sum_P(-1)^P\prod_{K=1}^{A}\psi_K(\vec{r}_{K_P}) \qquad (1)$$

The total wave function of many particle systems is written as a determinant of one-electron functions (spin-orbitals) [7]. Then the total wave function for three electron system is given by

$$\Psi=(3!)^{-1/2}\left|\varphi_{1s}\alpha(1)\varphi_{1s}\beta(2)\varphi_{nl}\alpha(3)\right| \qquad (2)$$

and for six electron system

$$\Psi=(6!)^{-1/2}\left|\varphi_{1s}\alpha(1)\varphi_{1s}\beta(2)\varphi_{2s}\alpha(3)\varphi_{2s}\beta(4)\varphi_{2p_x}\alpha(5)\varphi_{2p_y}\alpha(6)\right| \qquad (3)$$

where φ is the spatial part of the spin-orbital; and α and β refer to the two components of the spin part. The orbitals, in turn, are written as an expansion in some set of analytic basis functions

$$\varphi_{n,l}=\sum_i C_n^i\chi_{nl}^i \qquad (4)$$

n,l = (*1s, 3p)* or (*1s, 3d)*. The bas is functions χ are standard normalized Slater-type orbitals (STO's) and given by [7]

$$\chi_{n,l,m_l}(\vec{r},\theta,\phi,\xi)=R_n(\vec{r},\xi)Y_{lm_l}(\theta,\phi) \qquad (5)$$

Where

$$R_n(\vec{r},\xi)=\mathrm{N}\cdot r^{n-1}\cdot e^{(-\xi\cdot\vec{r})} \qquad (6)$$

and C_n represents the constant coefficient yield from the self consistent field (SCF) method, n is the principle quantum number, ξ is the orbital exponent, and N is a normalization constant given by [11]

$$N = \frac{(2\xi)^{n+1/2}}{[(2n)!]^{1/2}} \quad (7)$$

If (i,j) labels a pair of occupied φ_i and φ_j in the restricted HF description of the system, then the change, due to correlation in the (i,j) component of the second-order density $\Gamma_{ij}(\chi_m, \chi_n)$ which derived from the HF wave functions using the partitioning technique of Banyard and Mashat (1977) [12].

$$\Gamma_{ij}(\chi_m,\chi_n) = \frac{1}{2}[\varphi_i(\chi_m)\varphi_j(\chi_n) - \varphi_j(\chi_m)\varphi_i(\chi_n)] \quad (8)$$

To study the physical properties for a many particle systems, we must find the electron-pair density for each individual electronic shell, so

$$\Gamma(x_m, x_n) = \sum_{i<j}^{3} \Gamma_{ij}(x_m, x_n) \quad (9)$$

For any N-electron atomic system, the radial interparticle distribution function is defined in terms of the spin-free second order density matrix as [13.14]

$$f_{ij}(r_{12}) = \int \Gamma_{ij}(\vec{r}_1, \vec{r}_2) \frac{d\upsilon_1 d\upsilon_2}{dr_{12}} \quad (10)$$

where $\vec{r}_1$ represents the space coordinates of electron 1. The element of volume $d\upsilon_i$ is defined as $d\upsilon_i = r_i^2 \sin\theta_i d\theta_i d\phi_i d\vec{r}_i$.

$$r_{12}^2 = r_1^2 + r_2^2 - 2r_1 r_2 \cos\theta_{12} \quad (11)$$

one obtains

$$r_{12} dr_{12} = r_1 r_2 \sin\theta_{12} d\theta_{12} \quad (12)$$

provided that r_1, r_2 are kept fixed. The combined volume element therefore becomes [13]

$$\frac{d\upsilon_1 d\upsilon_2}{dr_{12}} = \vec{r}_1 \vec{r}_2 r_{12}\, d\vec{r}_1 d\vec{r}_2\, \sin\theta_1 d\theta_1 d\phi_1 d\omega \quad (13)$$

where ω denotes the angle of rotation given in Fig. 1.

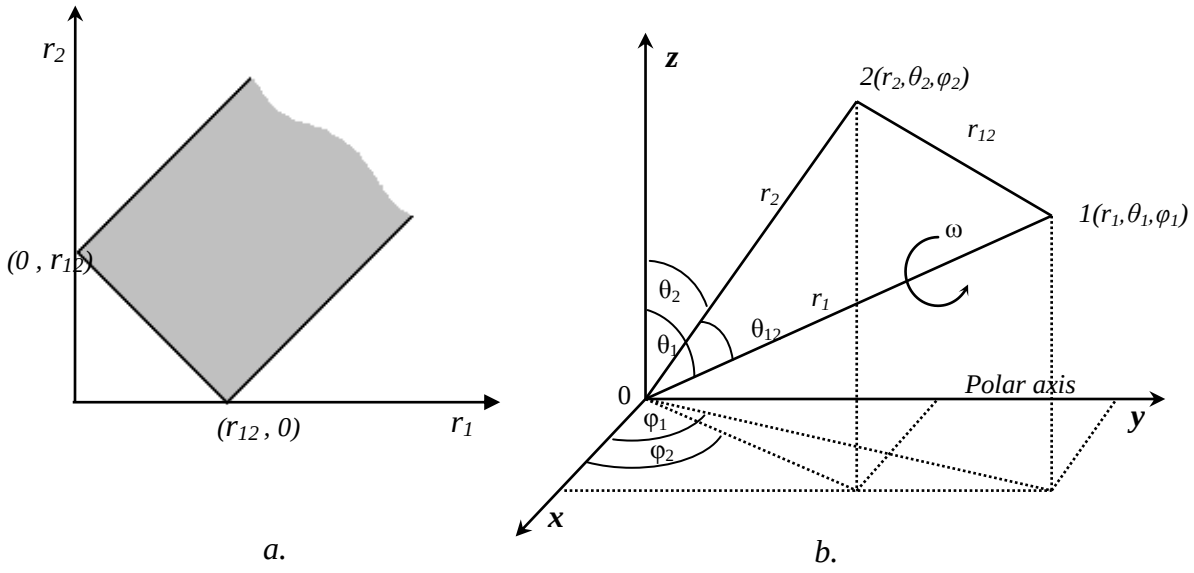

Fig. 1: a. The radial integration range in Equ.(3.10) is represented by the shaded area. b. Coordinate system involved in the determination of f(r_{12}). Here, r_1, r_2 are position vectors for electrons 1 and 2 relative to the origin point [13].

By substituting Equ.(13) into Equ.(10), we get [15]

$$f_{ij}(r_{12}) = r_{12}\int \Gamma_{ij}(\chi_1,\chi_2)\,\vec{r}_1\,\vec{r}_2\,d\vec{r}_1\,d\vec{r}_2\sin\theta_1\,d\theta_1\,d\phi_1\,d\omega \quad (14)$$

For the spherically symmetric case (*s*-orbital) where the azimuthal (or orbital) angular momentum quantum number $\ell = 0$, f*(r12)* can be evaluated from [13].

$$f(r_{12}) = 8\pi^2 r_{12}\left\{\int_0^{r_{12}}\vec{r}_1 d\vec{r}_1\int_{r_{12}-r_1}^{r_{12}+r_1}\Gamma(\vec{r}_1,\vec{r}_2)\,\vec{r}_2 d\vec{r}_2 + \int_{r_{12}}^{\infty}\vec{r}_1 d\vec{r}_1\int_{r_1-r_{12}}^{r_{12}+r_1}\Gamma(\vec{r}_1,\vec{r}_2)\,\vec{r}_2 d\vec{r}_2\right\} \quad (15)$$

In the present analysis the *2p*, *3p* and *3d* states are examples of non-spherically symmetric system. The expression for $f(r_{12})$ obtained from [16]

$$f(r_{12}) = r_{12}\left\{\int_0^{r_{12}}\vec{r}_1 d\vec{r}_1\int_{r_{12}-r_1}^{r_{12}+r_1}\Gamma_{12}(\vec{r}_1,\vec{r}_2)\,\vec{r}_2 d\vec{r}_2\times I + \int_{r_{12}}^{\infty}\vec{r}_1 d\vec{r}_1\int_{r-r_{12}}^{r_1+r_{12}}\Gamma_{12}(\vec{r}_1,\vec{r}_2)\,\vec{r}_2 d\vec{r}_2\times I\right. \quad (16)$$

In the foregoing, the distribution function $f(r_{12})$ is averaged over all positions of the two electrons. But we might ask what the distribution function would look like if one of the electrons is at a specified distance from the nucleus. If the position of electron 1 is specified as $\vec{r}_1$ then one can introduced a new distribution function which depends on r_{12} and $\vec{r}_1$ and given by [17]

$$g(r_{12},\vec{r}_1) = \vec{r}_{12}\,\vec{r}_1\int_{|r_{12}-r_1|}^{r_{12}+r_1}\Gamma_{ij}(\vec{r}_1,\vec{r}_2)\,\vec{r}_2\,d\vec{r}_2\times I \quad (17)$$

I represent the integrals of the most general type

$$I = \int Y_{\ell_1 m_1}(\theta_1,\phi_1)\,Y^*_{\ell_2 m_2}(\theta_1,\phi_1)\,Y_{\ell_3 m_3}(\theta_2,\phi_2)\,Y^*_{\ell_4 m_4}(\theta_2,\phi_2)\sin\theta_1 d\theta_1 d\phi_1 d\omega$$

I can be written as [10]

$$I = \frac{1}{2}(-)^{m_2+m_4}\sum_{\ell=|\ell_1-\ell_2|}^{\ell_1+\ell_2}\sum_{\ell'=|\ell_3-\ell_4|}^{\ell_3+\ell_4}\left[\frac{L_1L_2L_3L_4}{LL'}\right]^{\frac{1}{2}}\times C(\ell_1\,\ell_2\,\ell;m_1-m_2\,m)\,C(\ell_3\,\ell_4\,\ell';m_3-m_4\,m')$$

$$C(\ell_1\,\ell_2\,\ell;000)\,C(\ell_3\,\ell_4\,\ell';000)\times(-)^{m'}P_{\ell'}^{m'}(\cos\theta_{12})\,\delta_{\ell\ell'},\delta_{m-m'} \quad (18)$$

where

$C(\ell_1\,\ell_2\,\ell;m_1-m_2\,m)$ is the Clebsch-Gorden coefficient defined by [18], and is sometimes expressed in traditional notation $\langle \ell_1\,\ell_2\,m_1\,m_2|\,\ell_1\,\ell_2\,\ell\,m\rangle$, $L_i = 2\ell_i+1$, $m = m_1 - m_2$, $m' = m_3 - m_4$ and δ_{xy} is the Kronecker delta function.

Eq.(12) can be written in term of Wigner *3j* symbols by using the following relation

$$\langle \ell_1\,\ell_2\,m_1\,m_2|\,\ell_1\,\ell_2\,\ell\,m\rangle = (-1)^{-\ell_1+\ell_2-m}\sqrt{2\ell+1}\begin{pmatrix}\ell_1 & \ell_2 & \ell\\ m_1 & m_2 & -m\end{pmatrix} \quad (19)$$

The important properties and the values of Wigner 3j symbols were given and tabulated in Ref. [19]

The associated Fermi hole can be written as a difference between the electron-electron distribution function $f(r_{12})$ for triplet state (^3s) or (αα) and these for singlet state (^1s) or (αβ) [10]

$$\Delta f(r_{12}) = f_{KM(^3s)}(r_{12}) - f_{KM(^1s)}(r_{12}) \quad (20)$$

and the partial Fermi hole, $\Delta g(r_{12},r_1)$ is defined as the different between the partial distribution function $g(r_{12},r_1)$ for triplet and singlet state

$$\Delta g(r_{12},r_1) = g_{KM(^3s)}(r_{12},r_1) - g_{KM(^1s)}(r_{12},r_1) \quad (21)$$

Partial Fermi hole $\Delta g(r_{12},r_1)$ against (r_{12},r_1), enables us to study correlation effects when the test electron 1 is located at a given radial distance from the nucleus; the integral of $\Delta g(r_{12},r_1)$ against r_1 equals $\Delta f(r_{12})$.

Results and discussion

The probability of finding the inter-particle distribution function $f(r_{12})$ between electrons unlike and like spins in *KM* shell for Li-atom in the different excited states can be observed in the curves (A) and (B) presented in Fig. 2. For both states, at small r_{12}, the $f(r_{12})$ distribution function is influenced mainly by the electron pair behavior, since the outer electron cannot penetrates the K-shell, so we see a flat region. The absence of this feature is due to the difference in symmetry of the *1s* and *3p* and *3d* orbitals. In *1s 3p* state these curves indicates two principal maxima in each curve refer to the probability of finding the outer electron one in *2p* and the other in *3p*. For *1s 3p* state the maximum values of $f(r_{12})$ between electrons with like spin is greater than between electrons with unlike spin and the locations is less and vice versa for *1s 3d* state. The maximum values of $f(r_{12})$ for *1s 3d* > *1s 3p* and vice versa for its locations.

We now examine the inter-particle distribution function $f(r_{12})$ for inter-shells as $1s_\alpha\ 2p_\alpha$, $1s_\beta\ 2p_\alpha$, $2s_\alpha\ 2p_\alpha$ and $2s_\beta\ 2p_\alpha$ of the C-atom in Figs.(3) (a) and (b) for $1s_\alpha\ 2p_\alpha$, $1s_\beta\ 2p_\alpha$, $2s_\alpha\ 2p_\alpha$ and $2s_\beta\ 2p_\alpha$ which show the *2p* electrons cannot penetrated the *1s* or *2s* so we see a flat regions at small r_{12} and this regions for αα > βα because Fermi effect and the density of two electrons in parallel state larger than in singlet state in *1s 2p* but vice versa for *2s 2p*, the maximum values of $f(r_{12})$ for *1s 2p* > *2s 2p* and its locations for *2s 2p* > *1s 2p*. It can be seen that Fermi hole is plotted as a difference between $f(r_{12})$ of $K_\alpha\ M_\alpha$ shell (triplet state) and $K_\beta\ M_\alpha$ shell (singlet state) for Li-atom in the different excited states in Fig. 4 and for different states of C-atom in Fig. 5 which shows the depth of Fermi hole decreases and its radius increases when the outer electron excited to farther orbital in Li-atom and an increasing in the depth and radius of Fermi hole in *2s 2p* state compared with *1s 2p* state in C-atom, due the large distance between tow electrons in L-shell.

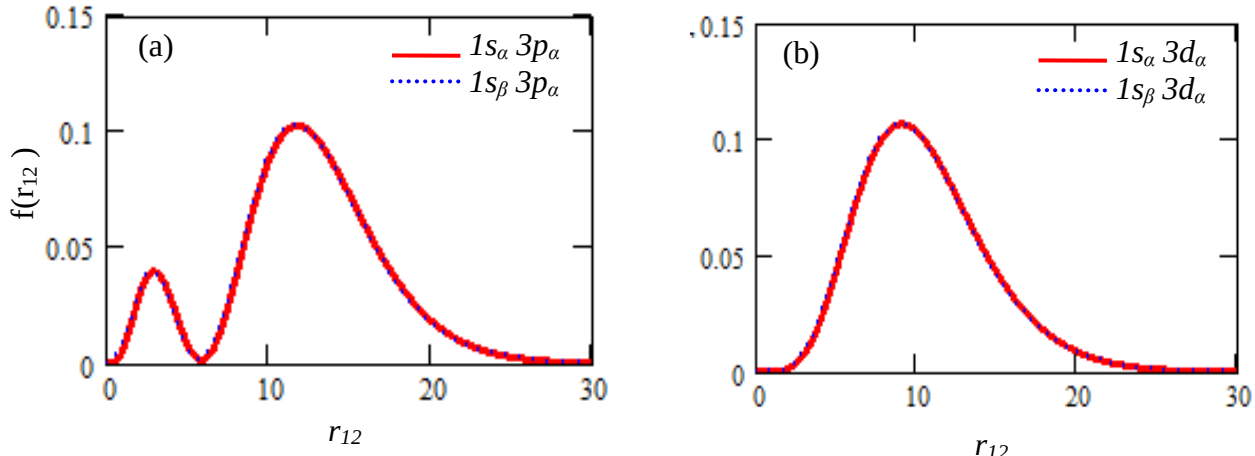

Fig. 2: The inter-particle distribution function $f(r_{12})$ for Li-atom in the different excited states (a) $1s_\alpha\ 3p_\alpha$, $1s_\beta\ 3p_\alpha$ and (b) $1s_\alpha\ 3d_\alpha$, $1s_\beta\ 3d_\alpha$.

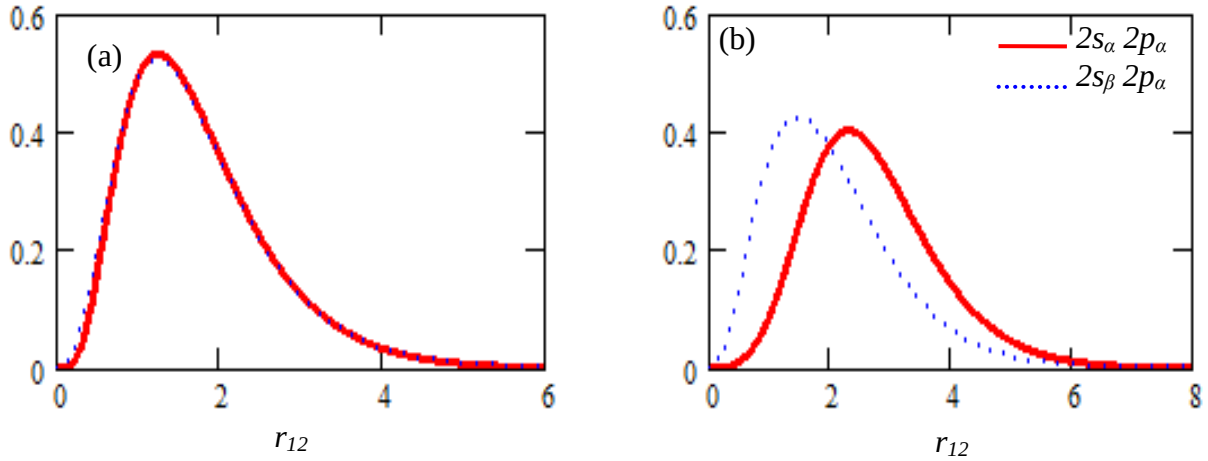

Fig. (3). The inter-particle distribution function $f(r_{12})$ for Li- atom in the different excited states (a) $1s_\alpha\ 2p_\alpha$, $1s_\beta\ 2p_\alpha$ and (b) $2s_\alpha\ 2p_\alpha$, $2s_\beta\ 2p_\alpha$.

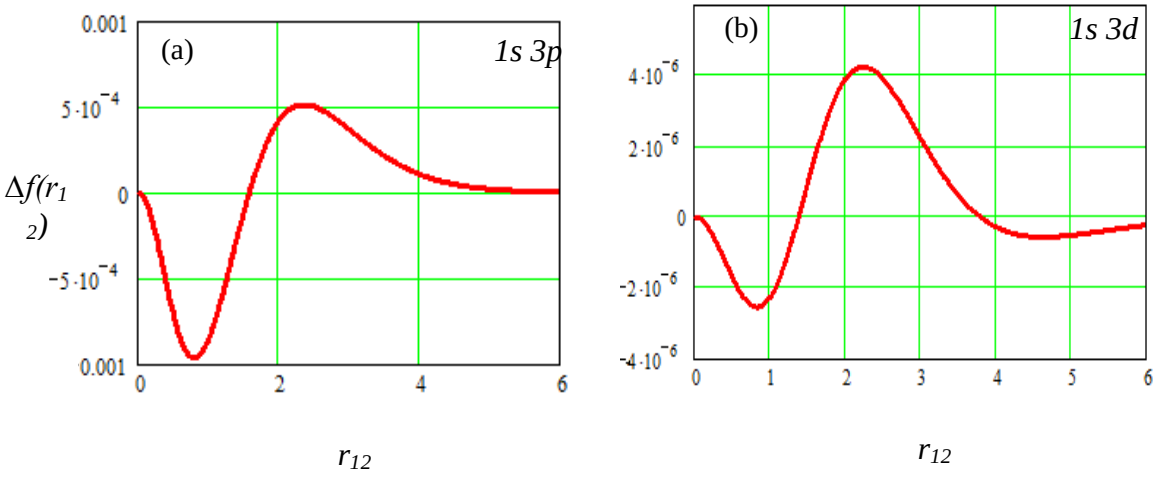

Fig. 4: The Fermi hole $\Delta f(r_{12})$ evaluated from $f_{\alpha\alpha}(r12)$-$f_{\beta\alpha}(r12)$ for Li- atom in different excited states (a) 1s 3p and (b) 1s 3d.

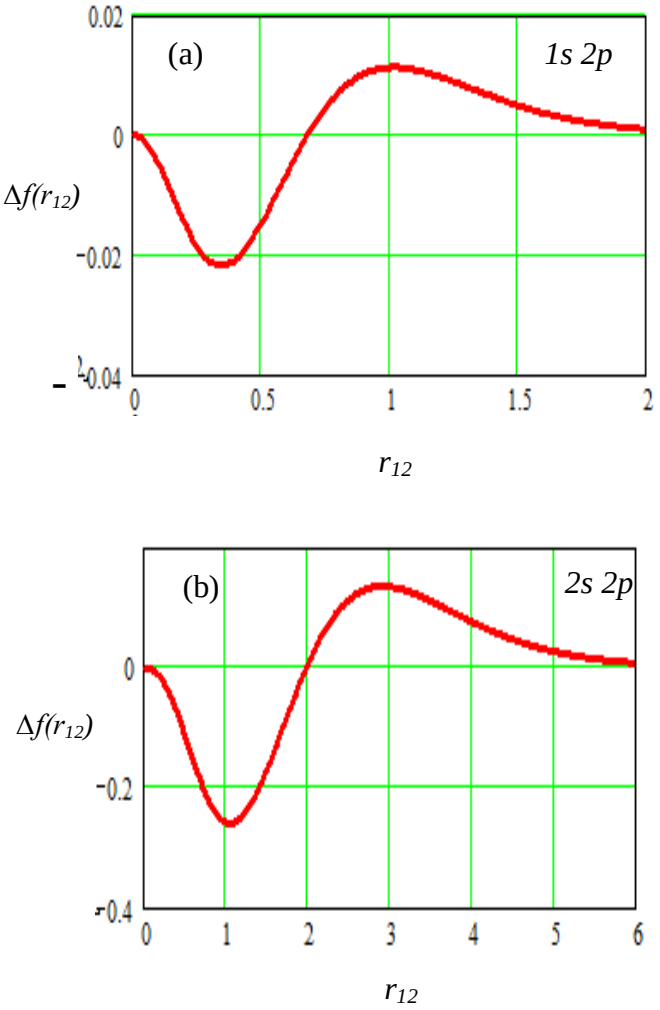

Fig. 5: The Fermi hole Δ f(r_{12}) evaluated from $f_{\alpha\alpha}(r12)$-$f_{\beta\alpha}(r12)$ for C-atom in different excited states (a) 1s 2p and (b) 2s 2p.

The $g(r_{12},r_1)$ diagrams (surfaces and contours) for $KM(^3s)$, $KM(^1s)$, $KL(^3s)$, $KL(^1s)$, $LL(^3s)$ and $LL(^1s)$ shells for Li- and C-atoms in states *1s 3p*, *1s 3d*, *1s 2p* and *2s 2p* in Figs. 6-9 respectively, show the change in behavior of the inter-particle probability functions as the position of the test electron is varied and show the same characteristics in the region of the diagonal $r_{12}=r_1$ axis, when r_1 is large compared with r_K. This similarity also holds for the features parallel to the r_{12} axis, when $r_{12} \rangle r_1 = r_K$. Such features are characteristic of an inter-shell distribution. In $1s_\alpha\ 3p_\alpha$- shell r_1 values represent the location of the three maxima for K-, L- and M- shell. In the diagonal structure, inspection of $g(r_{12}, r_1)$ confirms that at the maximum, when $r_1=r_M$, the value of r_{12} does indeed exceed r_1. Furthermore, for a given diagonal contour, the span of r_1 indicates the spreads of the L- and M-shells densities whereas, for a fixed choice of r_1, say $r_1 \approx r_M$, the range of r_{12} reflects the relative compactness of the K-shell density. Conversely, for the parallel feature, the ranges of r_1 and r_{12} relate to the K-, L- and M-shells distributions, respectively. Naturally, the Fermi effect produces negligible values of $g(r_{12},r_1)$ at small r_{12} for all r_1.

Distribution for $1s_\beta\ 3p_\alpha$-shell shows the characteristic diagonal and parallel features seen previously for $1s_\alpha\ 2p_\alpha$. However, since Fermi effect is not present in this instance, the mini K-shell effect does not appear in the $g(r_{12}, r_1)$ surface due to the different symmetry.

The same behavior can be seen in *1s 3d* state but there different existence in r_1 values represent the maxima of two probabilities of finding electron in K- and M-shell in because outer electrons cannot penetrates L-shell.

The $g(r_{12},r_1)$ diagrams (surfaces and contours) for $2s_\alpha\ 2p_\alpha$ and $2s_\beta\ 2p_\alpha$ sub-shells for C-atom have their main characteristics located about the $r_{12} \approx r_1$ diagonal line, and the maximum value for the density where $r_1 \approx r_{2p}$ and $r_{12} \approx r_{2s2p}$. As there is a very small effect parallel to the r_{12} axis represent the probability of permeation the *2s* electron to *1s* so $r_1 \approx r_{1s}$ and r_{12} represent the distance distributions between *1s* and *2p* sup-shell. In addition, and as expected, for every inter-shell.

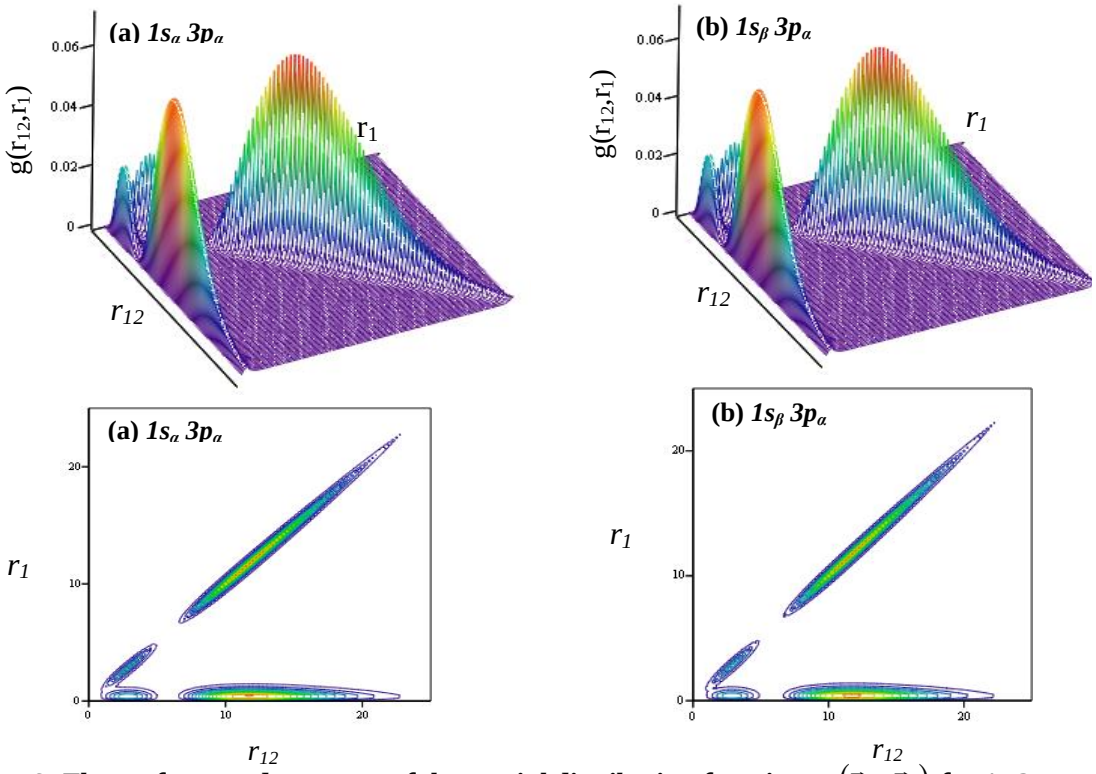

Fig. 6: The surfaces and contours of the partial distribution function $g(\vec{r}_{12},\vec{r}_2)$ for 1s 3p state of Li-atom in excited state ($1s^2 3p$), (a) $1s_\alpha\ 3p_\alpha$ and (b) $1s_\beta\ 3p_\alpha$.

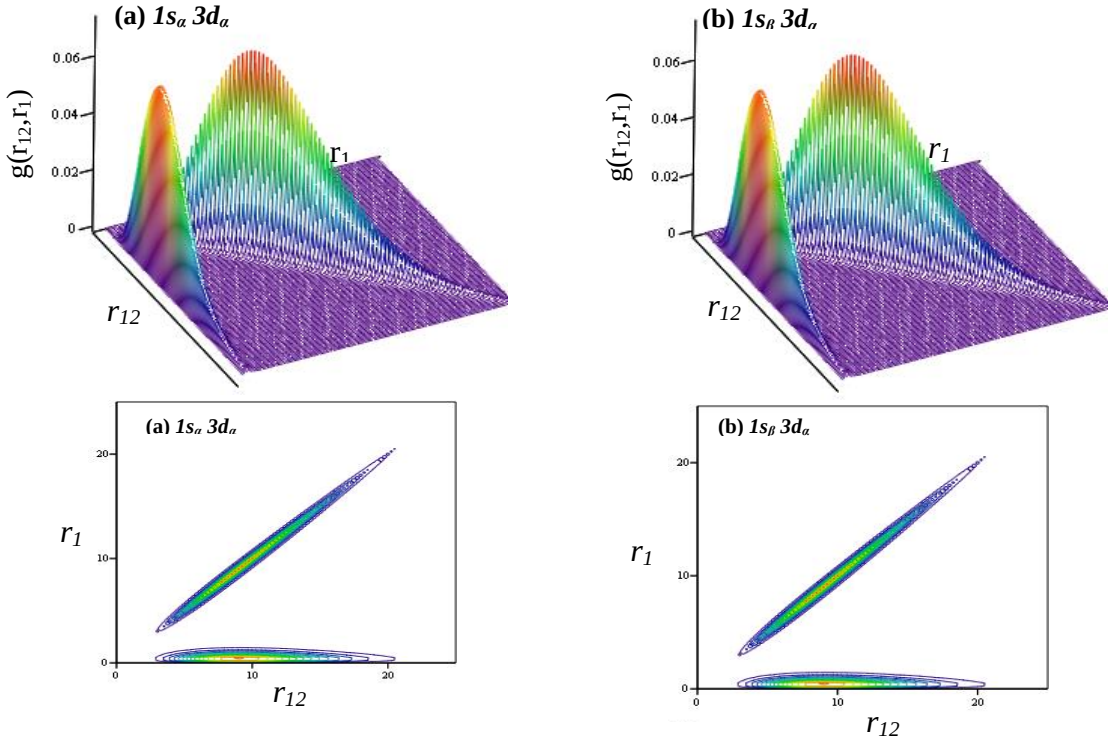

Fig. 7: The surfaces and contours of the partial distribution function $g(\vec{r}_{12},\vec{r}_2)$ for 1s 3d state of Li-atom in excited state ($1s^2 3d$), (a) $1s_\alpha\ 3d_\alpha$ and (b) $1s_\beta\ 3d_\alpha$.

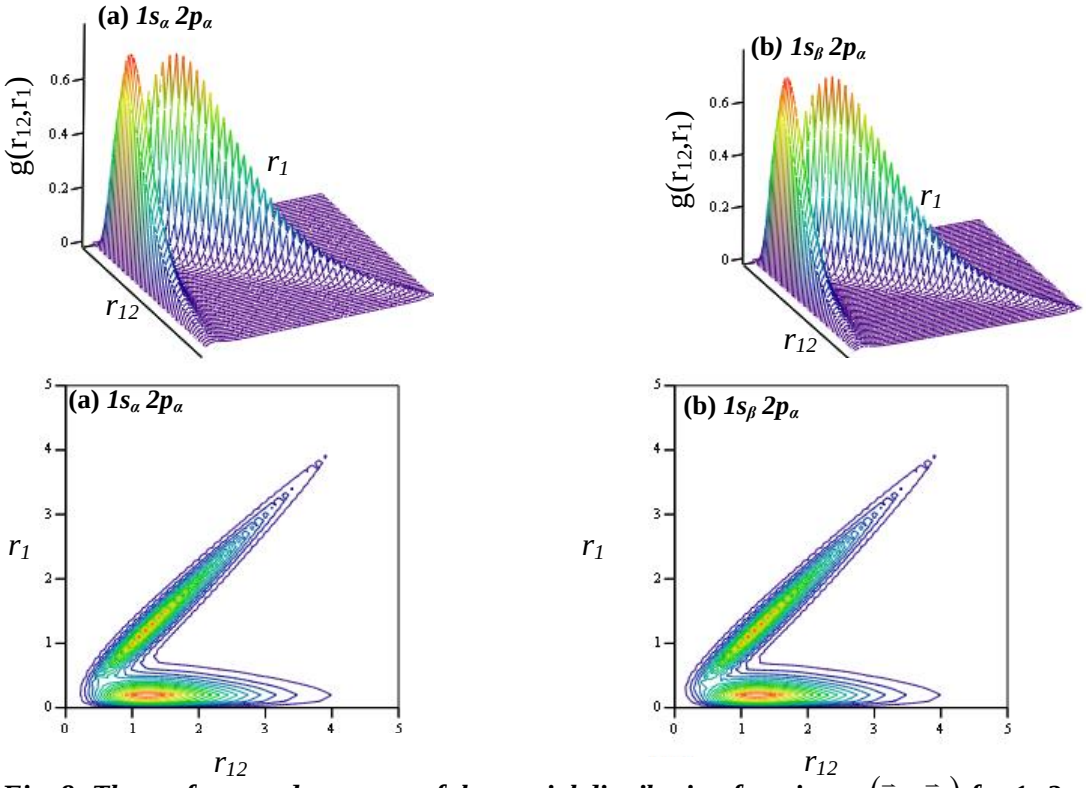

Fig. 8: The surfaces and contours of the partial distribution function $g\left(\vec{r}_{12},\vec{r}_{2}\right)$ ***for 1s 2p state of C-atom (a) 1s$_\alpha$ 2p$_\alpha$ and (b) 1s$_\beta$ 2p$_\alpha$.***

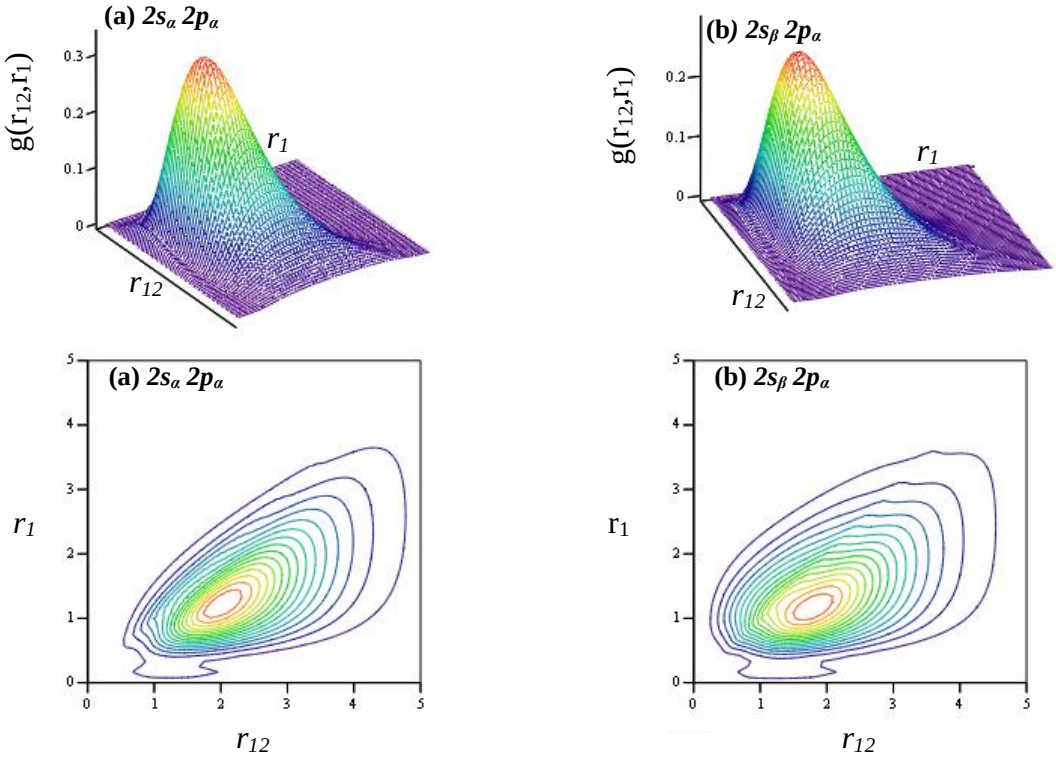

Fig. 9: The surfaces and contours of the partial distribution function $g\left(\vec{r}_{12},\vec{r}_{2}\right)$ ***for 2s 2p state of C-atom (a) 2s$_\alpha$ 2p$_\alpha$ and (b) 2s$_\beta$ 2p$_\alpha$.***

A partial Fermi hole as a difference between αα and βα for the selected systems of Li- and C-atom are plotted as surface and contour diagrams in Figs. 10 and 11 respectively. These Figures show that the depth of partial Fermi hole decreases and the radius increases as the outer electron excited to *3d* orbital in Li-atom and the depth as well as the radius of $\Delta g(\vec{r}_{12},\vec{r}_1)$ for *1s 2p < 2s 2p.*

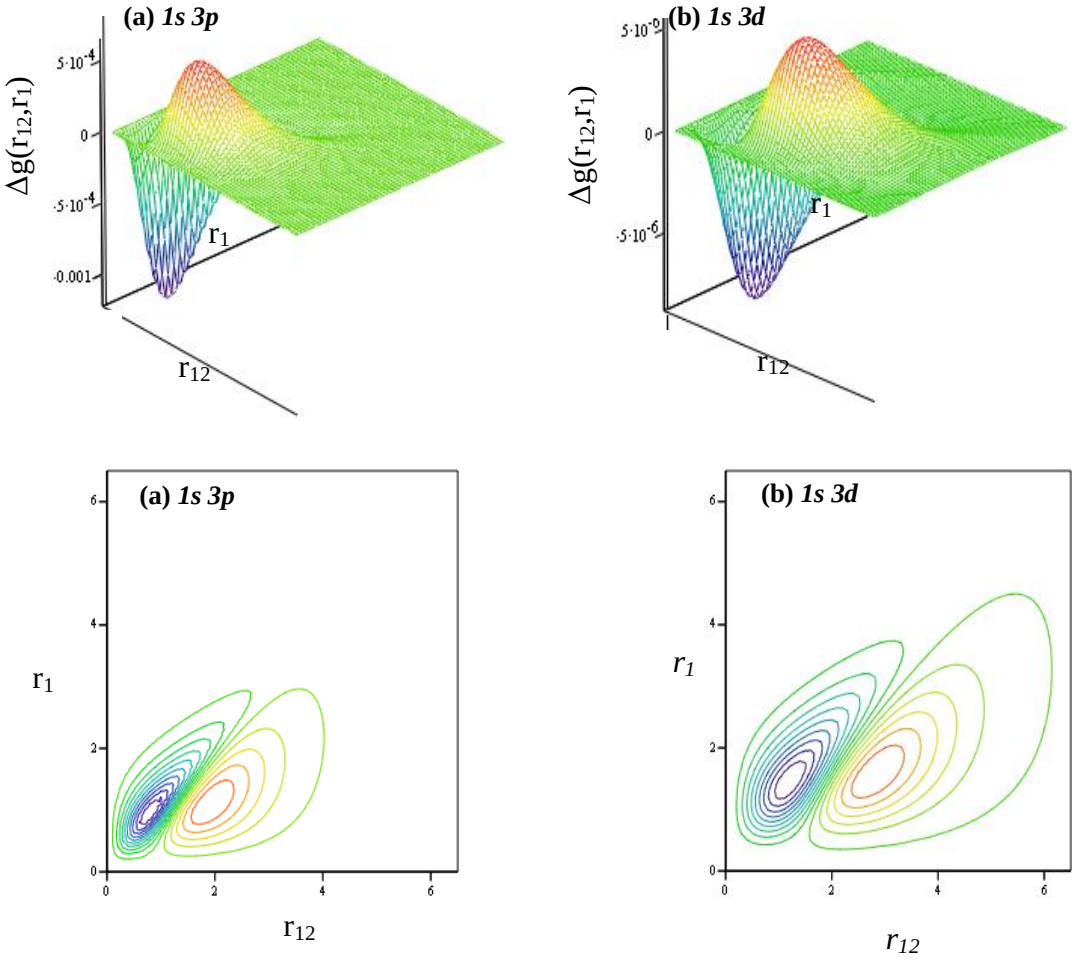

Fig. 10: The surfaces and contours of the partial Fermi hole $\Delta g(r_{12},r_1)$ evaluated from $g_{\alpha\alpha}(r_{12},r_1)$-$g_{\beta\alpha}(r_{12},r_1)$ for Li- atom in different excited states (a) 1s 3p and (b) 1s 3d.

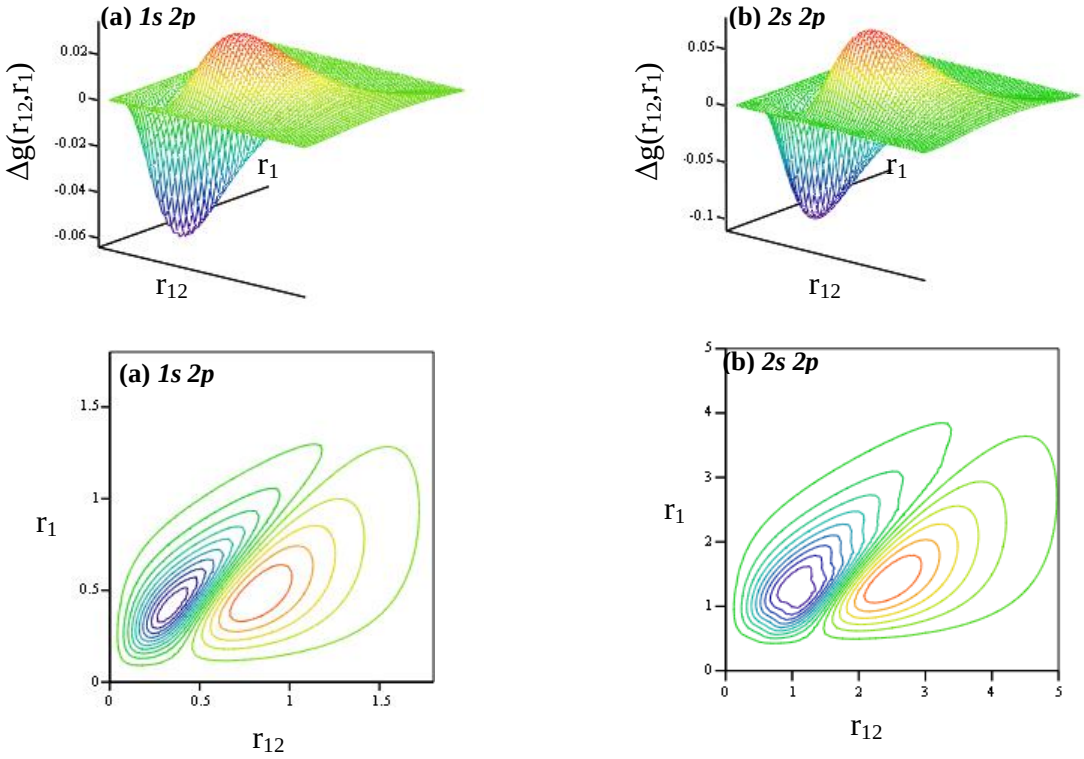

Fig. 11: The surfaces and contours of the partial Fermi hole $\Delta g(r_{12},r_1)$ evaluated from $g_{\alpha\alpha}(r_{12},r_1)$-$g_{\beta\alpha}(r_{12},r_1)$ for different states of C-atom, (a) 1s 2p and (b) 2s 2p.

Conclusions

From the present research, we deduce some notes for the inter-particle distribution function $f(r_{12})$, Fermi hole $\Delta f(r_{12})$, the partial density distribution function $g(r_{12},r_1)$ and partial Fermi hole $\Delta g(r_{12},r_1)$. When comparing the $f(r_{12})$ and $g(r_{12},r_1)$ for Li- and C-atoms in the different excited states, we see the maximum values for *1s 3d* are larger and their location the nearest to the nucleus from *1s 3p* in Li-atom and for *1s 2p* > *2s 2p* in C-atom, and a flat region in the small r_{12}. The depth of Fermi and partial Fermi hole decreases and the radius increases when the outer electron excited to further orbital. The depth of Fermi and partial Fermi hole for *2s 2p* is > *1s 2p* and vice versa for radius. As well as, penetration the orbitals by further orbitals electrons, occur only between orbitals are similar in spherical symmetry.

References

[1] R. J. Boyd, C.A. Coulson, J. Phys. B: Atom. Molec. Phys. 6 (1973) 782.
[2] V. W. Maslen, Proc. Phys. Soc. A 69 (1956) 734.
[3] G. Sperber, Int. J. Quantum Chem. 5 (1971)189.
[4] R. J. Boyd, C. A. Coulson, J. Phys. B: At Mol. Phys. 7 (1974) 1805.
[5] N. Moiseyev, J. Katriel, R. J. Boyd, J. Phys. B: At. Mol. Phys. 8 (1975) 130.
[6] K. H. Al-Bayati, PhD. Thesis, Leicester University (1984).
[7] A. W. Weiss, Astrophys. J. 138 (1963) 1262.
[8] M. A. Buijse, E. J. Baerends, Mol. Phy. 100 (2002) 401.

[9] D. Dill, Mechanics/ Fermi Holes and Heaps, Department of Chemistry Boston University, Boston MA02215 (2003).
[10] A. A. Alzubadi, Ph.D Thesis, University of Technology, Iraq (2005).
[11] J. Huang, Q. Zhao, G. Jiang, Commun. Theor. Phys. 5 (2010) 871.
[12] K. E. Banyard and M. M. Mashat, J. Chem. Phys. 67 (1977) 1405.
[13] C.A. Coulson, A. H. Neilson, Proc. Phys. Soc. 78 (1961) 831.
[14] S. Bubin and O. Prezhdo, Phys. Rev. Lett. 111 (2013) 193401.
[15] P. R. Dressel and F. W. King, J. Chem. Phys. 100 (1994) 7515.
[16] R. Benesch, Int. J. Quant. Chem. 6 (1972)181.
[17] R. J. Boyd, C. A. Coulson, J. Phys. B: Atom. Molec. Phys. 6 (1973) 782
[18] M. E. Rosse, "Elementary Theory of Angular Momentum" John Wiley and Sons, New York, (1967).
[19] R. D. Cowan, "The Theory of Atomic Structure Spectra" University of California Press, California, (1981).